Proceedings of the
Annual Stability Conference
Structural Stability Research Council
Grapevine, Texas, April 18-21, 2012

Assessment of buckling stability of elastically-braced castellated beams

H. Showkati[1], T. Ghanbari Ghazijahani[2], A. Noori[3], T. Zirakian[4]

Abstract
Castellated beams have been widely used in buildings based on their structural, constructional, and economical advantages. The widespread use of castellated beams, on one hand, and the presence of the web openings in these structural elements resulting in various failure modes, on the other hand, has prompted several investigations into their structural behavior, and in particular, a proliferation of research work has been undertaken on buckling stability of such beams. Despite the numerous reported studies on the structural stability and performance of castellated beams, no experimental study has been reported on the bracing requirements of these flexural members against lateral buckling. Hence, in the present study the behavior of elastically-braced castellated beams subjected to pure bending has been investigated experimentally. The experimental results and findings have been evaluated by considering some analytical solutions as well as the AISC 360-10 code requirements and predictions.

1. Introduction

Castellated beams have been widely used in multistory buildings, commercial and industrial buildings, warehouses, and portal frames based on their structural, constructional, and economical advantages. Castellated beams are fabricated from standard profiles by splitting a rolled beam along its web in a zig-zag pattern and then rejoining the two halves by welding. This results in a deeper beam which is stronger and stiffer than the original one. In fact, as a result of castellation process the overall beam depth is increased by 50%, while the weight of the beam is kept constant. The main advantages of fabrication as well as application of castellated beams may be listed as following (Srimani Sri and Das 1978, Zirakian and Showkati 2006):

- Use of lighter beams, which results in saving of material and handling cost;
- Use of beams with high strength-to-weight ratio;
- Eliminating the need for heavy built-up beams;
- Use of the web openings for duct work and piping;

[1] Department of Civil Engineering, Urmia University, Urmia, Iran, <h.showkati@urmia.ac.ir>
[2] Department of Civil Engineering, Mahabad Branch, Islamic Azad University, Mahabad, Iran, <tohidghanbari@gmail.com>
[3] Department of Civil Engineering, Bu-Ali Sina University, Hamedan, Iran, <nori.amir@gmail.com>
[4] Department of Civil and Environmental Engineering, University of California, Los Angeles, U.S.A., <tzirakian@ucla.edu>

- Optimum utilization of the existing profiles; and
- Easy-fabrication of tapered sections.

The presence of the web openings in castellated beams results in various failure modes at the perforated sections. A survey of the literature reveals that various theoretical and experimental studies have been carried out over the last three decades on the structural stability and performance of castellated beams and different failure modes *viz.* the Vierendeel collapse mechanism, buckling of a web post, web-weld failure, lateral-torsional and lateral-distortional types of buckling, *etc.* have been identified and investigated. Lateral-torsional buckling of these members was studied by Nethercot and Kerdal (1982). Web buckling of castellated beams was also studied theoretically and experimentally by Redwood and Demirdjian (1998) and Zaarour and Redwood (1996). Later on, lateral-distortional buckling of castellated beams was identified and studied experimentally by Zirakian and Showkati (2006). In addition, the bracing requirements of castellated beams were studied recently by Mohebkhah (2003) and Mohebkhah and Showkati (2005) through finite element analyses.

Despite the numerous published studies, no experimental study has been reported on the bracing requirements of castellated beams against lateral buckling. Hence, the structural behavior of elastically-braced castellated beams subjected to pure bending is investigated in this experimental study. Experimental results are compared with some analytical solutions and evaluated by considering the AISC 360-10 (2010) code requirements and predictions.

2. Test details and findings

The schematic representation of the test rig and overall view of the test setup are provided in Figs. 1 and 2, respectively. As it is shown in the figures, the test rig consisted of loading and supporting components, elastic bracing system, and the full-scale castellated test beam which are described in the following.

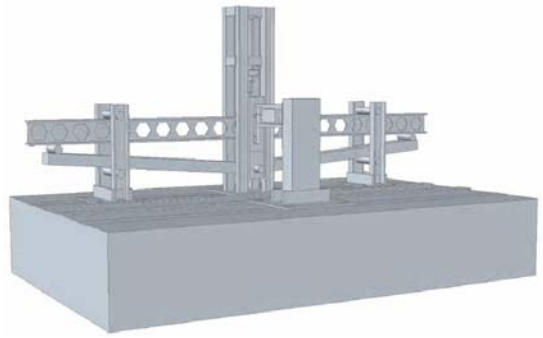

Figure 1: Schematic representation of the test rig

Figure 2: Overall view of the test setup

The test specimens were loaded by means of a 608 kN hydraulic jack. The hydraulic jack was mounted vertically on a strong bearing frame which, in turn, was anchored to a steel deck strongly fixed on a concrete floor. The load was applied through a steel box with a proper opening through which the castellated beam was passed. The steel box was fixed on a steel loading saddle underneath with a hole drilled in it for placing a shaft. The shaft passed through both steel loading saddle and the Rigid Inclined Loading Arms (RILAs), and allowed the RILAs to rotate around its center during the loading process, so that the central zone of loading system

acted as a hinged point. The two ends of the RILAs with the aid of the special boundary conditions, applied pure bending through two concentrated loads which made a couple at the two ends of the castellated beam. The details of the loading system are shown in Figs. 1, 2, and 3.

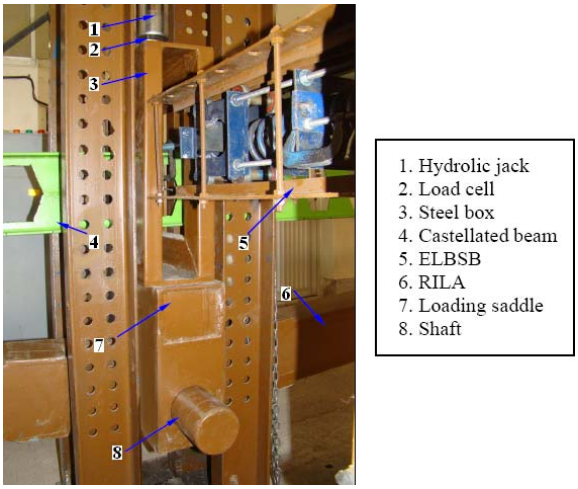

Figure 3: Components of the loading systems

Figs. 4(a) and (b) show the details of the end supports. As seen in Fig. 4(a), two ball-bearings and a shaft were used at these boundary zones. The upper fixed ball-bearing was placed on the upper flange of the castellated beam and the lower one was installed under the RILA, while the shaft was located on the upper surface of the RILA with a certain horizontal distance from the ball-bearings. In addition, as seen in Fig. 4(b), beam lateral bracing at the end supports was provided by means of four ball-bearings (two at each side) and two plates devised on both sides of the beam.

(a) Ball-bearings and the shaft at the end support

(b) Lateral bracing at the end support

Figure 4: Details of the end supports

Details of the midspan lateral bracing system are illustrated in Fig. 5. This novel system was indeed designed to study the buckling behavior of elastically-braced I-section beams. By considering the functionality of this bracing system, it was called as “Elastic Lateral Bracing System of Beams”, which is referred to as ELBSB in this paper.

1. Main body of the bracing system
2. Ball-bearing
3. Adjusting plate
4. UNP profile
5. Bracing hinged contact element
6. Rolling box
7. Bolt
8. Spring

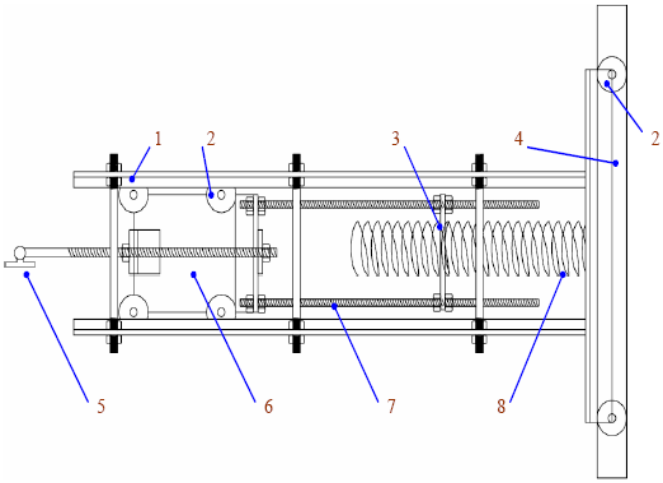

(a) Components of the ELBSB

(b) Overall view of the ELBSB

(c) Bracing of top flange

Figure 5: Details of the midspan lateral brace

As it is seen in Figs. 5(a), (b), and (c), the bracing system consisted of various components. An axial coil spring was used as the main component of the ELBSB which was placed and fixed on a UNP100 element. Four ball-bearings were devised on the UNP section allowing the whole ELBSB to move vertically during the in-plane vertical displacement of the test specimens. On the other hand, the spring was connected to the rolling box in order to move horizontally. Note that eight ball-bearings were connected to the rolling box to let it move without friction and hindrance. In addition, the spring was surrounded by a plate with a circular cutout in a certain zone to adjust the stiffness of the spring in such a way that the plate was fixed at a certain loop of the spring to provide the desirable stiffness. The surrounding plate was connected to the rolling box by means of four long bolts. The bracing arm of ELBSB, which was connected to the rolling box, was attached to the upper flange of the test beams. As shown in Fig. 5(c), the end of the bracing arm was designed in such a way that the contact of the ELBSB and the specimen was hinged to allow the beam to freely rotate at the restrained zone.

As listed in Table 1, test specimens consisted of nine 4.8 m long and full-scale castellated beams fabricated from the hot-rolled “IPE12” and “IPE14” profiles in accordance with the German Estahl Standard. Geometrical properties of the test specimens are illustrated in Fig. 6.

Table 1: Test specimens

CIPE12 test specimens	CIPE14 test specimens
CB 180-38.38	CB 210-38.38
CB 180-61.4	CB 210-61.4
CB 180-76.76	CB 210-87.7
CB 180-102.32	CB 210-153.5
CB 180-153.5	

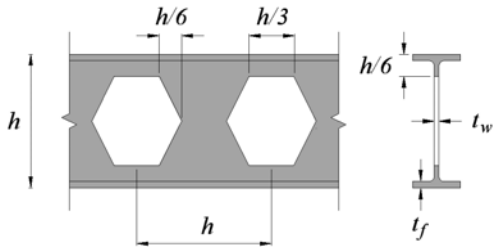

Figure 6: Geometrical properties of castellated beams

The labels of the test specimens were selected such that the overall height and the lateral bracing stiffness were considered. For instance, CB 180-87.7 implies that overall height of the castellated beam is 180 mm and the lateral bracing stiffness is 87.7 N/mm.

Material yield strengths were obtained from tensile coupon tests, which are summarized in Table 2. Furthermore, Young's modulus (E) and shear modulus (G) were taken as 206.01 GPa and $0.385E$, respectively.

Table 2: Material yield strengths obtained from tensile coupon tests

Test specimen	Yield strength (MPa)	
	Flange	Web
CB 180	279.31	233.93
CB 210	280.29	332.03

A proper and efficient data acquisition system was employed to record the applied load as well as the developed displacement and strain values throughout the tests. A KYOWA-type digital load cell with the capacity of 50 kN and located under the hydraulic jack arm was used for recording the values of the applied load during the experiments. KYOWA-type digital LVDTs were also used to capture the lateral displacements at mid-length and quarter points of the beam span. Moreover, YEFLA-5-type strain gauges were used to record the values of the strains developed at the aforementioned locations. All of the test data were collected and processed by a KYOWA-type digital data logger, a scanner, and a software called as UCAM-20PC.

Loading was performed in a step-by-step and incremental manner and the behavior of the specimen was thoroughly monitored during the test through visual inspections and assessment of the captured data. Based on the experimental observations, the buckling mode of the specimens with lower restraint stiffness was a half-sine wave with the maximum lateral displacement at the midspan, whereas in stiffer lateral bracing cases, the maximum lateral displacement was mostly

observed at the quarter points of the total span as shown in Fig. 7. Some sample moment-displacement/strain curves are shown in Figs. 8 and 9.

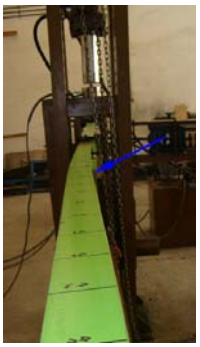

Figure 7: Lateral buckling of test specimens

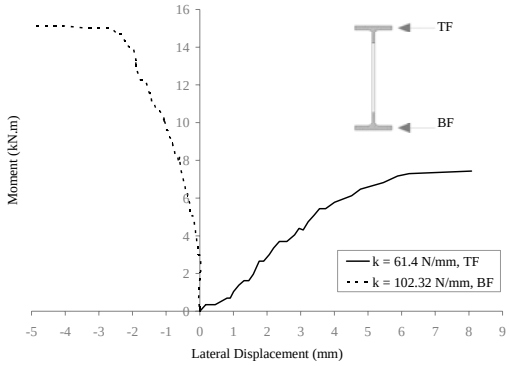

Figure 8: Lateral displacements at quarter points of *CB 180* with different midspan brace stiffnesses

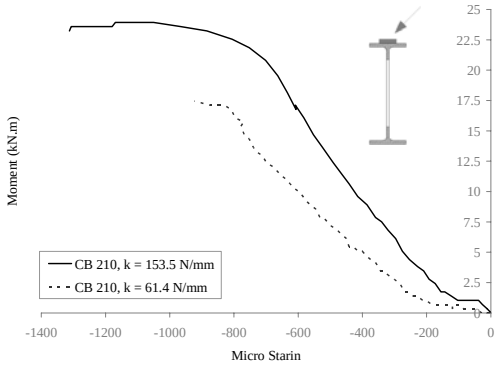

Figure 9: Strains developed at the center of the top flange at quarter point

From the figures it is evident that due to the occurrence of buckling instability at a certain load level, the specimen loses its load-bearing capacity and the deformation characteristics, *i.e.* lateral displacement and strain, tend to increase considerably. Moreover, as seen, specimens with a stiffer midspan lateral brace exhibit a larger buckling capacity. This is because of effectiveness of the midspan lateral brace in lowering the unbraced length of the beam.

3. Comparison with analytical solutions

The experimental buckling moments are compared with the analytical predictions of a design equation developed by Yura (Yura and Phillips 1990) for discrete or continuous lateral bracing of beams as follows

$$M_{cr} = \sqrt{(M_o^2 + \frac{P_y^2 h_o^2 A}{4}) \times (1 + A)} \qquad (1)$$

where

$$M_0 = \frac{\pi}{L}\sqrt{EI_y GJ + \frac{\pi^2 E^2 I_y^2 h_o^2}{4L^2}}, \tag{2}$$

$$A = \frac{L^2}{\pi}\sqrt{\frac{0.67 c_L \beta_L}{EI_y}}, \tag{3}$$

$$P_y = \frac{\pi^2 EI_y}{L^2}, \tag{4}$$

and

$$c_L = \frac{1}{1 + 1500\dfrac{\Delta_o}{L}}. \tag{5}$$

In the above equations, β_L is the equivalent continuous lateral brace stiffness, c_L is a reduction factor for the imperfection, and Δ_o is the initial imperfection value. Eq. (1) applies only to compression flange bracing, since lateral bracing becomes ineffective when placed at a distance below the compression flange (Yura and Phillips 1990). In order to determine the equivalent continuous brace stiffness (β_L) in Eq. (3), the stiffness of the single discrete brace at midspan of each test specimen was divided by 75 percent of the beam length as recommended by Yura and Phillips (1990). Furthermore, Δ_o was set equal to $L/1000$ in theoretical calculations. Experimental and analytical results are given in Fig. 10.

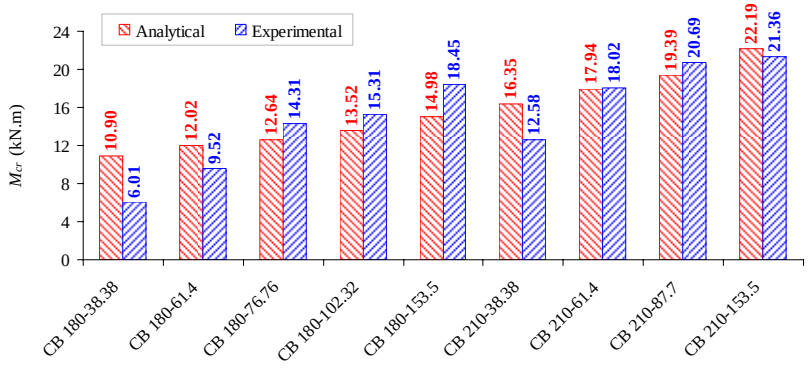

Figure 10: Experimental results and analytical predictions of Eq. (1)

As it is seen in the figure, the agreement between the experimental and analytical results is generally satisfactory. This indicates that Eq. (1) yields reliable predictions for the buckling moment of laterally-braced beams. In case of CB 180 specimens, Eq. (1) overestimates the buckling capacity at lower stiffness values, while as the lateral brace stiffness increases, analytical predictions lay below the experimental results. In case of CB 210 specimens a similar trend is also observed, however the experimental and theoretical results seem to be relatively

well-correlated in this case. As a whole, the findings of this study demonstrate that Eq. (1) may be confidently used for estimating the buckling capacity of laterally-braced beams; nonetheless, its accuracy can be still improved by considering more experimental and numerical results.

4. AISC 360-10 code requirements and predictions

The experimental results of the current study are also evaluated by considering the AISC 360-10 (2010) code requirements and predictions. Appendix 6 in AISC 360-10 (2010) addresses the minimum strength and stiffness necessary to provide a braced point in a column, beam or beam-column. AISC 360-10 (2010) addresses the "relative" and "nodal" bracing systems for beams with lateral bracing. In contrast to a relative brace system, a nodal brace controls the movement at the braced point without direct interaction with adjacent braced points. In the current experimental setup, a nodal lateral brace system was applied and its effectiveness is investigated herein.

According to AISC 360-10 (2010), the required nodal bracing stiffness is

$$\beta_{br} = \frac{1}{\phi}\left(\frac{10M_r C_d}{L_b h_o}\right), \tag{6}$$

where $\phi = 0.75$, $C_d = 1.0$ for bending in single curvature, and M_r is the required flexural strength which is determined by Eq. (2) herein. As shown in Fig. 11, the required brace stiffnesses for the 4.8 m CB 180 and CB 210 specimens are calculated using Eq. (6) and compared with the experimental brace stiffnesses.

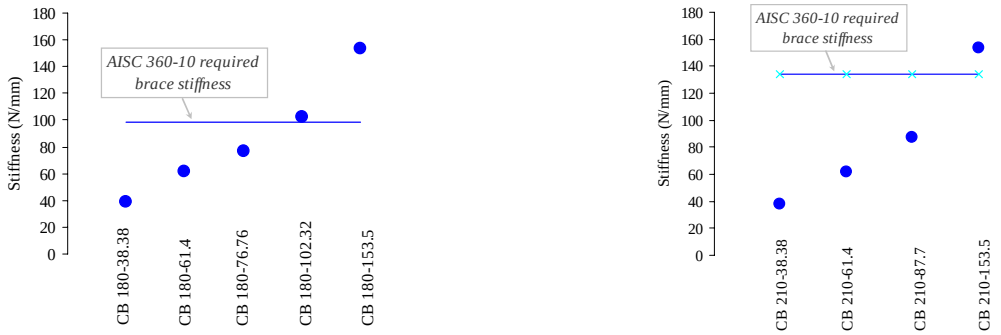

(a) CB 180 (b) CB 210)

Figure 11: Experimental and AISC code-required lateral brace stiffnesses

As it is observed in the figures, the experimentally-applied 102.32 and 153.5 N/mm brace stiffnesses in case of CB 180 (Fig. 11(a)) and 153.5 N/mm brace stiffness in case of CB 210 (Fig. 11(b)) are larger than the code requirements; therefore, the lateral displacement of the top compression flange at midspan is expected to be effectively controlled in these cases compared to those with lower stiffness values. In fact, this was verified by the test results and observations and the beam was effectively braced against lateral deformations.

The experimental buckling moments are compared with those predicted by the AISC code equations. According to the AISC 360-10 (2010) code specifications, the flanges and webs of CB 180 and CB 210 specimens are considered as compact, and the specimens were expected to undergo elastic lateral buckling. The nominal lateral-torsional buckling strength (M_n) is calculated for beams with half-span and full-span lengths by considering the effect of the midspan lateral brace, since test beams with lower midspan lateral brace stiffness underwent lateral-torsional buckling with a half-sine-wave mode, while as the stiffness of the midspan lateral brace was increased the beams exhibited a complete-sine-wave buckling mode. In Figs. 12(a) and (b), the buckling moments are plotted against the lateral brace stiffness values for CB 180 and CB 210 test specimens, respectively.

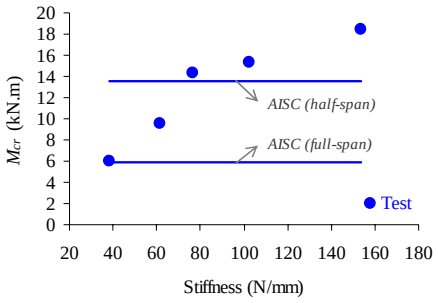

(a) CB 180

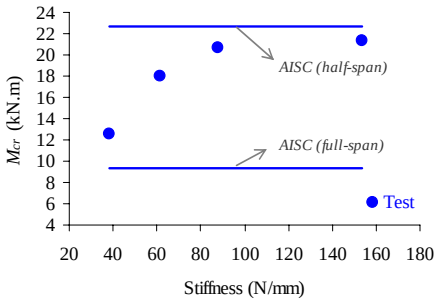

(b) CB 210

Figure 12: Comparison of test results and AISC code predictions

As it is seen in Figs. 12(a) and (b), at lower stiffnesses test results are in general close to the code predictions for the full-span length, while as the brace stiffness increases they tend to approach the predictions with half-span-length consideration. In case of CB 180 specimens (Fig. 12(a)), test results tend to lay beyond the code predictions with half-span-length consideration as the brace stiffness increases and code equations seem to yield conservative predictions. In contrast, in case of CB 210 specimens (Fig. 12(b)), test results lay between the two extreme cases of full-span and half-span lengths over the entire range of brace stiffness values.

As a whole, by considering the effects of various factors in theory and test, the agreement between the experimental results and code predictions is found to be fairly satisfactory. It should be noted that consideration of the reduced cross-section properties of the castellated beams in theoretical calculations may result in slightly conservative predictions. Also, arrangement of initial geometrical and material imperfections and interaction between the buckling behaviors of the two adjacent unbraced spans as well as the restrained midspan section may affect the buckling capacity of the beam in the experiment. In any case, it is believed that consideration of further experimental and numerical results can result in more optimal and effective code equations and rules.

5. Conclusions

Nine full-scale and simply supported castellated beams subjected to pure bending with a central elastic restraint were tested and reported in the paper. Based on the experimental observations, test specimens with lower lateral brace stiffness exhibited a half-sine-wave buckling mode with a

mid-length maximum out-of-plane deflection, while enhanced brace stiffness resulted in increased buckling capacity and a complete-sine-wave buckling mode with the maximum out-of-plane deflections at the span quarter points. Despite the theoretical considerations and test conditions, the agreement between the test results and predictions of the other analytical approaches was found to be by and large satisfactory. Evaluation of the experimental results and findings also revealed that the subject of lateral bracing of structural members seems to be satisfactorily addressed by the AISC 360-10 code; nevertheless, further experimental and theoretical research can still improve the efficacy of the code provisions.

References

AISC 360-10 (2010). "Specification for Structural Steel Buildings." *American Institute of Steel Construction*, Chicago, IL.

Mohebkhah, A. (2003). "Nonlinear lateral-torsional buckling of castellated beams with an elastic lateral restraint using FEM." *M.Sc. Thesis*, Dept. of Civil Engineering, Urmia University, Iran.

Mohebkhah, A., Showkati, H. (2005). "Bracing requirements for inelastic castellated beams." *Journal of Constructional Steel Research*, 61 (10) 1373-1386.

Nethercot, D.A., Kerdal, D. (1982). "Lateral-torsional buckling of castellated beams." *The Structural Engineer*, 60B (3) 53-61.

Redwood, R., Demirdjian, S. (1998). "Castellated beam web buckling in shear." *Journal of Structural Engineering*, ASCE, 124 (10) 1202-1207.

Srimani Sri, S.L., Das, P.K. (1978). "Finite element analysis of castellated beams." *Computers & Structures*, 9 (2) 169-174.

Yura, J.A., Phillips, B.A. (1990). "Bracing requirements for elastic steel beams." *M.Sc.Eng. Thesis*, The University of Texas at Austin, USA.

Zaarour, W., Redwood, R. (1996). "Web buckling in thin webbed castellated beams." *Journal of Structural Engineering*, ASCE, 122 (8) 860-866.

Zirakian, T., Showkati, H. (2006). "Distortional buckling of castellated beams." *Journal of Constructional Steel Research*, 62 (9) 863-871.